PAPER ID 10.18462/iir.gl.2018.1264

WATER TO WATER HEAT PUMP WITH MINIMUM CHARGE OF PROPANE

Klas Andersson[(a)], Eric Granryd[(b)], Björn Palm[(c)]

[(a)] Klas Andersson Engineering
Lidingö, 18161, Sweden, klas@ka-e.se
[(b)] Professor emeritus, The Royal Institute of Technology,
Stockholm, 10044, Sweden, eric.granryd@energy.kth.se
[(c)] Professor, The Royal Institute of Technology,
Stockholm, 10044, Sweden, bjorn.palm@energy.kth.se

ABSTRACT

This paper describes the technology for an environmentally friendly ground source heat pump for a single family home, characterized by using pure water as coolant and propane as refrigerant. The objective was to build a test system, operating under realistic conditions, using less than 150 g of propane, providing at least 5 kW heating capacity with reasonable efficiency and without freezing the coolant water.
The borehole heat exchanger was of coaxial type, providing about half the thermal resistance compared to a standard U-tube collector (Acuña 2010).
The evaporator and condenser where asymmetrical plate heat exchangers with small channel height (< 1 mm) on the refrigerant side. They were developed and manufactured exclusively for this project with a new type of press pattern, including a special, small volume sub-cooling section at the end of the condenser. A DC-motor scroll compressor for AC in electric vehicles was used, characterized by small internal volumes, small oil charge and wide capacity range (800-9000 rpm). A PAG-type oil was used, which however seemed to cause some problems with heat transfer and pressure drop in the evaporator.
The system also included a specially built mini channel liquid/suction line heat exchanger and a standard thermostatic expansion valve.
The paper presents test results for a heating capacity range of 2-10 kW. The performance was reasonable in this range with a charge of 100 g of propane ($-1<T_2<5$°C, $30<T_1<55$°C). The charge that is required is determined at the lowest capacities, at low compressor speed and high evaporating pressures. A lower charge is beneficial at higher capacities.

Keywords: Heat pump, Propane, Minimum charge, Heat exchangers

1. INTRODUCTION

This project is based on experiences from earlier studies at the Royal Institute of Technology (Fernando et al, 2008) where mainly heat exchangers for minimum charge of propane were studied. This time all components and the total charge were considered. The project overall objective was to use best practice technologies to build an environmentally friendly ground source heat pump. To achieve this, components from different fields of refrigeration and some new developments were merged together in the system.
Beside focus on the system energy efficiency, two main environmental concerns are to 1) avoid anti-freeze additives in the coolant and 2) to use "natural" refrigerants.
In an earlier research project (Acuña, 2010) a coaxial borehole collector concept was developed and evaluated using pure water as coolant. The measured borehole resistance was about half compared with a standard U-tube collector. Such a collector is used in the present system.
Many of the refrigerants used today have high GWP-factors and often systems have relatively large charge of refrigerant. Many natural alternatives, like propane, are flammable. As pointed out by many authors (IIR 25th info. note, 2014) reducing refrigerant charge will be important for most systems. Beside the low density, propane has shown to be a good refrigerant in many aspects. (Pavel, 2014).
According to EN378 it is recommended to have a total charge of less than 150 g of ASHRAE class A3 refrigerants (like propane, R290) to avoid aggravating complications in terms of size, location and/or

ventilation of the space of installation. Less than 150 g of charge thus make a huge simplification since most potential hazardous situations then can be taken care of within the system boundaries. An example how to do this is given in IEC60335-2-40. The main focus in the project has therefore been to investigate how far we can reach in terms of small charge of R290. Initially the goal was to reach 5 kW heating capacity with less than 150 g. As the project developed it became clear that it was possible to reach higher capacities. The system was consequently rebuilt in steps to allow tests up to 10 kW heating capacity. Along this journey it was not possible to upgrade all components; particularly the evaporator was too small for high capacities.

2. THE SYSTEM

The system was built and installed in a house outside Stockholm and was operated in different configurations during one heating season. As a consequence, the measurement set up did not hold laboratory quality in terms of measurement accuracy. Also, the possibility to control operation conditions were limited by the characteristics of the house and borehole.

The condenser water circuit was thermally connected to the radiator system via a warm water heat exchanger. Both the condenser and radiator water flow rate were adjustable. By adjusting the radiator flow rate, the condenser water temperature could be set without changing the water flow rate through the condenser. The coolant water flow rate was adjustable but then the water flow through the evaporator was also changed. The layout is illustrated in Figure 1.

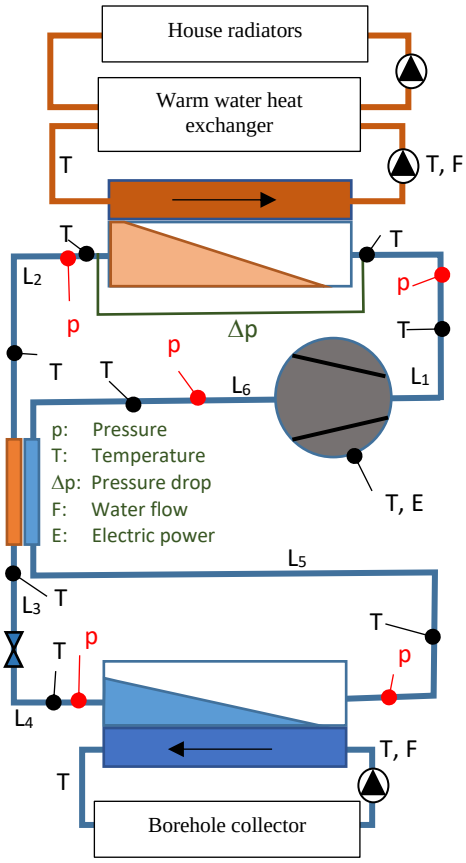

Figure 1. System layout and measurement configuration

2.1 Connection lines

In Table 1 the dimensions of the connection tubes are given together with calculated pressure drop, expressed as saturated temperature difference and calculated refrigerant hold up.

As a consequence of short connecting tubes, the temperatures measured can be influenced by heat conduction from adjacent components. To reduce that problem stainless steel tubes where used for lines L_2 and L_3 shown in Figure 2.

2.2 Expansion device

A standard thermostatic expansion valve was used in parallel with a manual metering valve, see Figure 3. The latter to be able to extend the capacity range. The internal volume of the expansion valve connections was reduced by introducing more narrow tubes. The bulb was mounted on L_6, after the suction line heat exchanger, while the pressure connection was at the evaporator outlet line L_5.

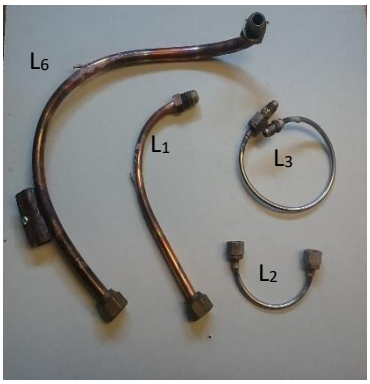

Figure 2. Connection lines. L_6 and L_1 with immersed temperture pockets. L_2 and L_3 ss-tubes without. L_6 with fitting for expansion valve bulb.

Figure 3. Manual valve (upper) and thermostatic valve (lower) in parallel. Connection lines L_4 and L_5.

Table 1. Connection lines

	Di mm	Length m	$\Delta T_{sat}(\Delta p_{sat})$ °C[a]	Charge g[a]
L_1	7.8	0.40	0.05	0.5
L_2	3.0	0.13	0.13	0.4
L_3	3.0	0.25	0.24	0.7
L_4	6.3	0.20	0.53	0.4
L_5	11.0	0.60	0.08[b]	1.6[c]
L_6	11.0	0.50	0.06	0.5

[a] Q_2=4.8kW T_1=40°C T_2=2.5°C
[b] quality=1 [c] quality ~ 0.97

2.3 Accesories

There was no sight glass, refrigerant receiver or filter dryer in the system. The refrigerant pressure was measured at five positions and one differential pressure meter was connected over the condenser with narrow capillary tubes in the positions illustrated in Figure 1.

2.4 Suction gas-liquid line heat exchanger, SucHex

The SucHex was made by pressing copper tubes into a flat shape and soldering them together, including connections as illustrated in Figure 4. The dimensions and calculated characteristics are given in Table 2 and 3 respectively. The heat balance over the SucHex was used to calculate the vapor quality at the evaporator outlet.

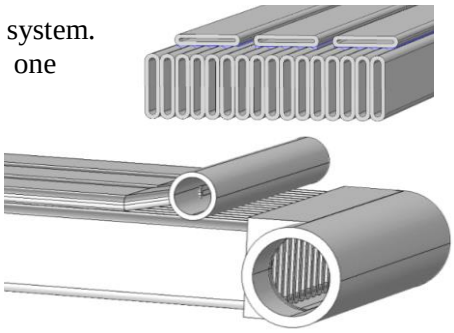

Figure 4. SucHex tube arrangement. Cut view of channels(upper) and connection assembly (lower).

Table 2. Suchex dimensions

	Vapor	Liquid
Height [mm]	1.2	0.6
Width [mm]	10	10
Length [mm]	300	260
Number of channels	16	3
Connection diameter [mm]	11	4.65

Table 3. Calculated SucHex characteristics

Q_1=4.8kW T_1=40°C T_2=2.5°C ΔT_{sup}=4K ΔT_{sub}=4K	Vapor	Liquid
Charge hold up, including connections [g]	1.1	4.1
Channel pressure drop* [Pa]	1100	6100
Temperature effectiveness	0.58	
Arrangement	counterflow	
*In/outlet losses and connections not included.		

2.5 Compressor

The compressor is a semi hermetic Sanden SHS33 scroll type with permanent magnet DC motor. The inverter drive and control electronics are integrated within the compressor and the motor is cooled by the suction gas. It has a small built-in oil separator and some other built-in protections. It is developed for use in air conditioning in electric vehicles. The required lifetime in vehicle AC-applications is normally much shorter than for residential heat pumps. The compressor comes with a PAG-type of oil which has low solubility of propane. Some characteristics are given in Table 4 and the main body dimensions in Figure 5. The total amount of oil in the system was less than 50 g during testing.

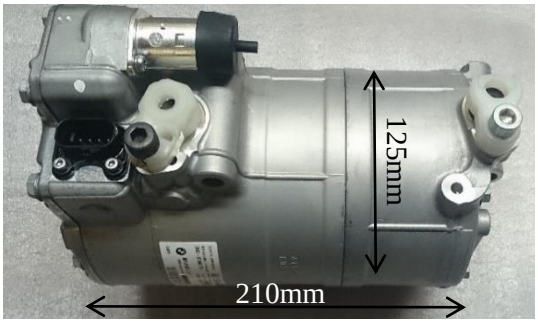

Figure 5. Sanden SHS33 compressor main body dimensions.

Table 4. Compressor characteristics

Swept volume [cm^3/turn]	33
Speed range [rpm]	800-9000
Suction side volume [cm^3]	500
Discharge side volume [cm^3]	260
Oil type	PAG–SPA2
Oil charge [cm^3]	<50
Weight [kg]	6.85

2.6 Evaporator and condenser

The heat exchangers are specially developed and manufactured for this project. They are brazed plate heat exchangers with a variety of press patterns. The pattern and press depth, and thereby the channel height, is different for the water and refrigerant side respectively. An extensive work was initially done with mapping how small press depth that can be used. Test plates with a range of press depths were made and soldered. They were then cut apart and the channels were checked for clogging solder - see example in Figure 6. A channel height with large margin to both clogging and pressure drop was selected and therefore there is potential for further reduction of the channel height. The condenser has a special sub-cooling section with small channel dimensions for large sub-cooling per refrigerant charge. Some basic data and estimated charge are given in Table 5.

Figure 6. Cut section of test plates where solder wetting was examined.

The inlet port of the evaporator was made relatively large in order to allow a distributor to be inserted.

Initially the system and heat exchangers were made for 5 kW heating capacity. It was then rebuilt to meet the requirements for 10 kW. A new condenser, with 24 instead of 19 channels was used but there was no time to make a new evaporator. The one used is too small for 10 kW.

For patent reasons it is not yet possible to give any further details about the channel geometries, other than that the channel height on the refrigerant side is less than 1 mm.

Table 5. Evaporator and condenser characteristics

	Evaporator	Condenser
Number of refrigerant channels	14	24
Heat transfer area [m^2]	0,68	1,04
Plate width x length [mm]	73 x 350	73 x 350
Estimated total charge[a] [g]	22.8[b]	52.3[c]

[a] Q_2=4.8kW T_1=40°C T_2=2.5°C $T_{sup}=T_{sub}$=4K [b] Hughmark correlation
[c] Remaining to sum up to total charge

2.7 Borehole collector

A 190-m deep, 115-mm diameter borehole served as heat source of the system, see Figure 7. A thin lining (0.4 mm) or "hose" is inserted in the hole and filled with fresh water up to just above groundwater level, pressing the "hose" towards the wall, giving good thermal contact. The coolant is circulated towards the bottom of the hole by a PE-tube (outer/ inner diameter 40/35.2 mm) reaching 168 m depth. The tube has an insulation along its upper half length to reduce thermal short circuiting. This concept was earlier evaluated by Acuña (2010) with thermal response test and fiber optic temperature measurements.

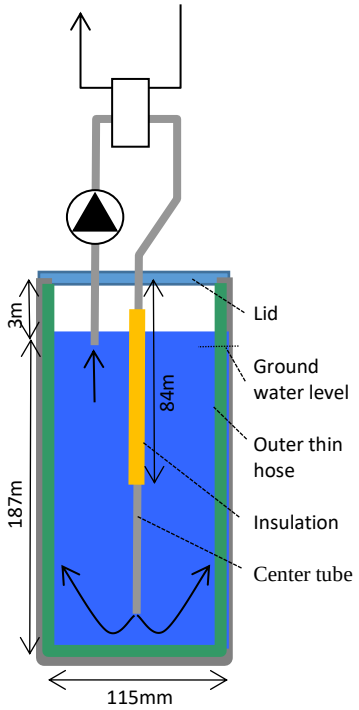

Figure 7 Collector principle

3. TEST SETUP

To keep internal volumes low, connecting tubes were short and narrow and therefore some temperature sensors were not positioned in pockets immersed in the flow. Along line L_2, L_3 and L_4 according to Figure 1, the sensors were mounted with aluminum tape flat against the tube outer surface.

Temperatures in the heat pump refrigerating circuit were measured with type T thermocouples. The evaporating saturation temperature was calculated from the pressure measured at the evaporator outlet. The condenser ditto was calculated from the pressure measured at the condenser inlet. The radiator and coolant temperatures and flow rates were measured with Brunata type HGS systems with immersed Pt-100 temperature sensors. The cooling and heating capacities were calculated from Brunata flows and temperatures using water properties from NIST RefProp 9.1.

The temperatures measured with the thermocouples, the Brunata Pt-100 sensors and calculated from pressures are estimated to be within ±0.5°C. This defines the accuracy of some performance figures.

The coolant water inlet temperature from the borehole was 7.0 to 9.0°C and the flow rate was 2535±10 liter/hour. The pressure drop on the water side was recorded to 19 kPa.

The condenser water flow rate was 985±15 liter/hour during the tests and the water pressure drop was 3,2 kPa.

The compressor is supplied from 230VAC via a full bridge (4 diodes) rectifier and a smoothing capacitor. The loss in the rectifier is included in the compressor input power measured with a DIZ W1E4 meter. The compressor speed could be set between 800 and 9000 rpm. The total amount of refrigerant charge was measured with a scale (Kern PCB 6000-1, with 0.1-g resolution). The refrigerant bottle, placed on the scale was connected with a spiral winded capillary tube to the system connections to ensure that no tension forces affected the reading during filling.

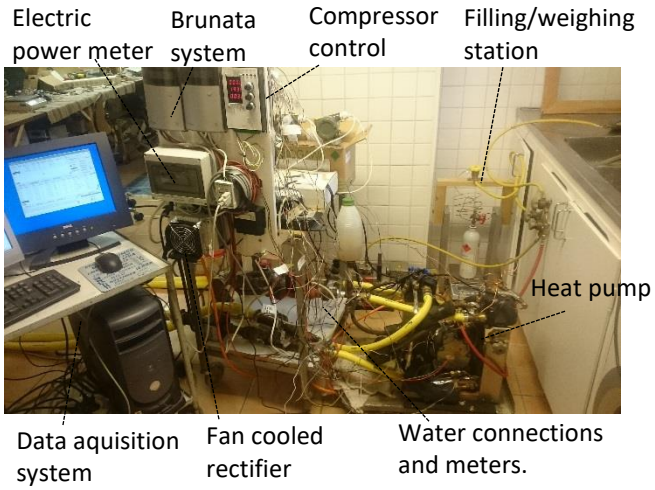

Figure 8. Test setup

4. RESULTS

4.1 Optimum charge

The superheat setting of the expansion valve was varied for different refrigerant charges at 2835 rpm constant compressor speed. For each setting and charge the condenser water outlet temperature was adjusted to be 40°C. It was not possible to control the coolant inlet temperature during the test series, why it slowly decreased from 8.2°C at beginning when the charge was 93 g, to 7.1°C at the end when the charge was 106 g. For each charge the expansion valve was adjusted for the highest $COP_1=Q_1/E_k$. In Figure 9 the results are plotted. Also shown is the corresponding system Carnot efficiency, defined from the condenser and evaporator *water outlet* temperatures. The Carnot system efficiency aims to compensate for the variation in the coolant temperature. A slight difference as to optimal charge for best efficiency appears.
The variation in *efficiency* with the charge is thus small. Also for the *capacity* the same is true as illustrated in Figure 10. It is hard to identify a true optimum.

The System Carnot efficiency is here defined by the cooling coefficient of performance, $COP_2= Q_2/E_k$, as:
$\eta_{Carnot_w,out} = \frac{COP_2}{COP_{2Carnot,w,out}}$ where $COP_{2Carnot,w,out} = \frac{T_{evap,w,out}}{T_{cond,w,out}-T_{evap,w,out}}$
The heat pump coefficient of performance $COP_1= Q_1/E_k$ is thus: $COP_1 =1+\eta_{Carnot,w,out} \cdot COP_{2Carnot,w,out}$

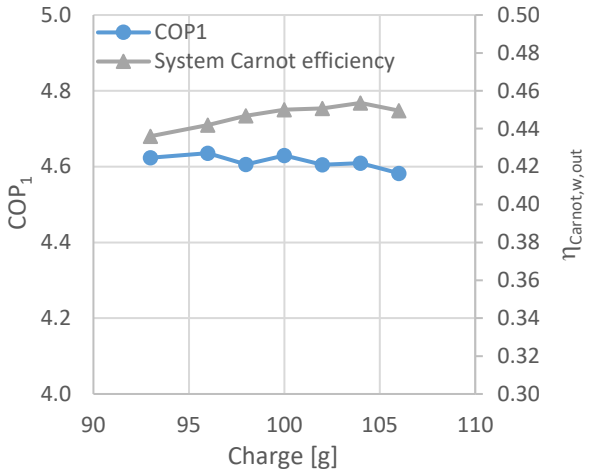

Figure 9. COP_1 and System Carnot efficiency. For conditions, see text.

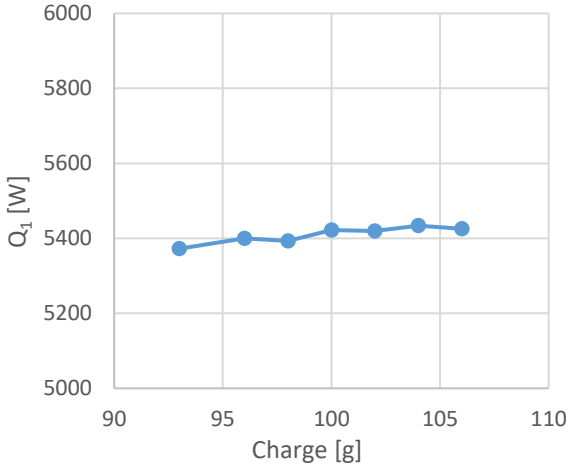

Figure 10. Heating capacity. For conditions, see text.

4.2 Optimum superheat and sub-cooling

The superheat after the evaporator from the optimum charge test series are shown in Figure 11 - 12. The COP_1 as function of superheat is illustrated in Figure 11. Notice that for this system the superheat is directly related to the sub-cooling in the condenser, as illustrated in Figure 12. The explanation for this is that different superheat influences the amount of refrigerant in the evaporator, which in turn has an effect on the amount in the condenser. A superheat of 4-5K gives maximum COP_1 for this system. There are complex reasons for this that need further analysis to explain. (A more optimal way of control might possibly be to control the amount of sub-cooling.)

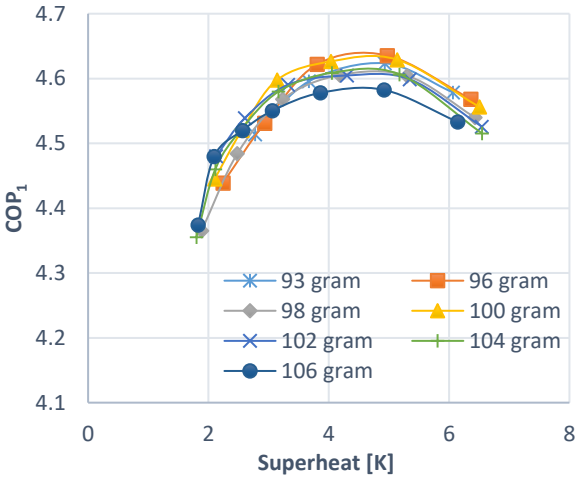

Figure 11. Optimum superheat..

4.3 Evaporator outlet quality

From a heat balance over the SucHex the change of vapor quality of the gas could be estimated. Assuming superheated and dry vapor after the SucHex, the evaporator outlet vapor quality was calculated as illustrated in Figure 13. At the superheat for maximum COP_1, 4-5K, the quality appears to be close to 0.97.

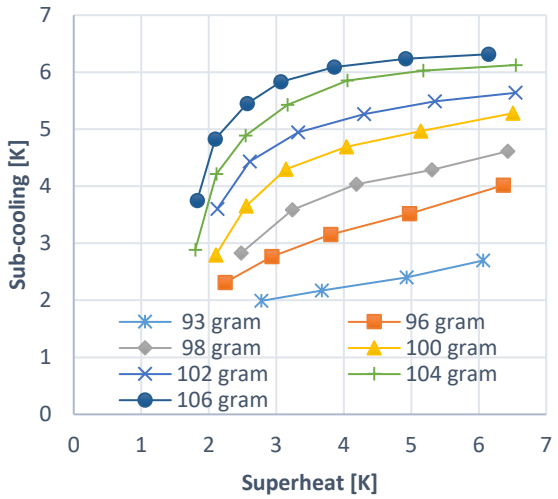

Figure 12. Charge distribution expressed as sub-cooling vs. superheat.

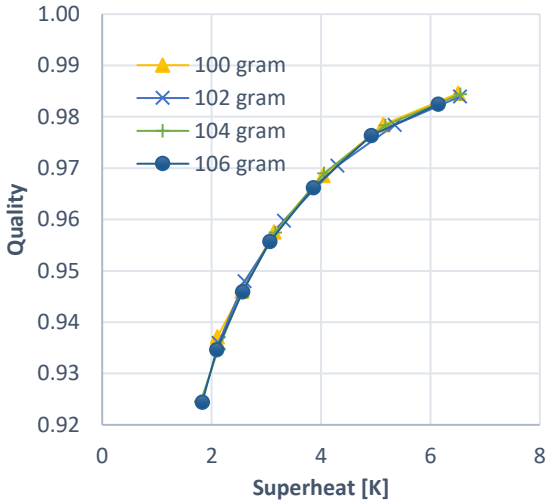

Figure 13. Vapor quality at evaporator outlet calculated from heat balance over the SucHex.

4.4 Charge distribution

Approximate charge distribution over the components was calculated from known interior volumes, to sum up with the measured total charge. The properties were defined at measured system state conditions using NIST RefProp 9.1. The vapor quality along the evaporator was calculated in steps from inlet conditions and heat balance with the measured water flow rate and average UA-value. The void fraction in each section was calculated using the Hughmark correlation (Hughmark,1962) from which the masses were calculated and summarized.

The quality at the evaporator outlet was taken into account when calculating the charge in the evaporator outlet and SucHex vapor lines. The result of such a distribution calculation for 100 g of total charge is illustrated in Figure 14.

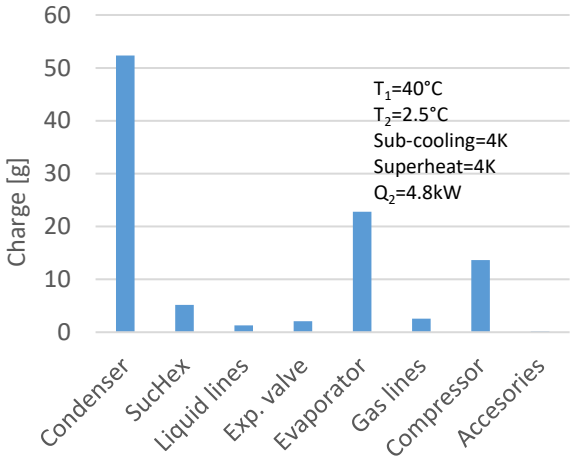

Figure 14. Calculated distribution of 100 g total charge.

4.5 System characteristics

The system was operated at different condenser water temperatures for a range of compressor rpm:s as illustrated in Figure15. The corresponding compressor power, including rectifier and inverter drive losses is given in Figure 16.

Figure 17 shows the relation between sub-cooling and superheat for the corresponding data points. The sub-cooling increases with the capacity (or rpm) which indicates that there is an excess of refrigerant at the highest rpm. The opposite is true at low rpm.

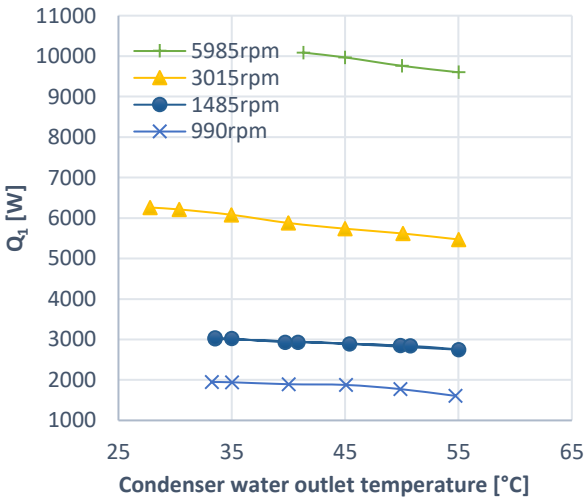

Figure 15. Heat capacity vs condenser water outlet temperature at different compressor speeds. Total charge 100 g.

4.6 Component characteristics

The characteristic of the evaporator and condenser is given as the differences between saturation temperature and water temperatures vs capacity in Figure 18 and 19 respectively.

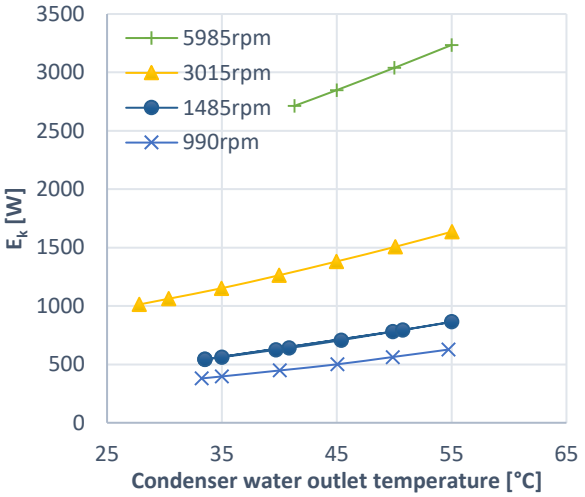

Figure 16. Compressor power vs condenser water outlet temperature at different compressor speeds. Total charge 100 g.

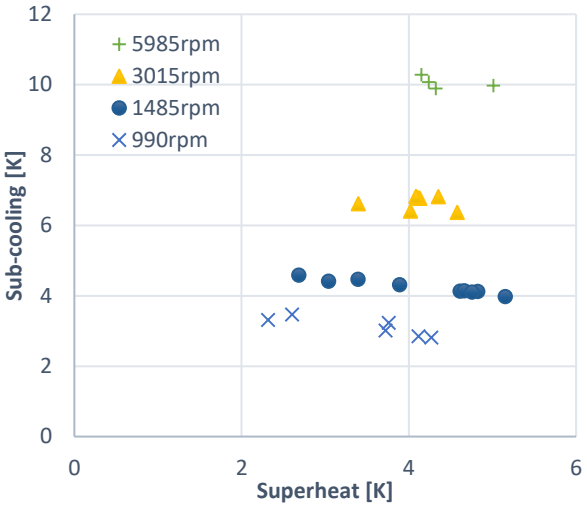

Figure 17. Illustration of excess of charge at high capacities (and lack of charge at low capacities). Total charge 100 g.

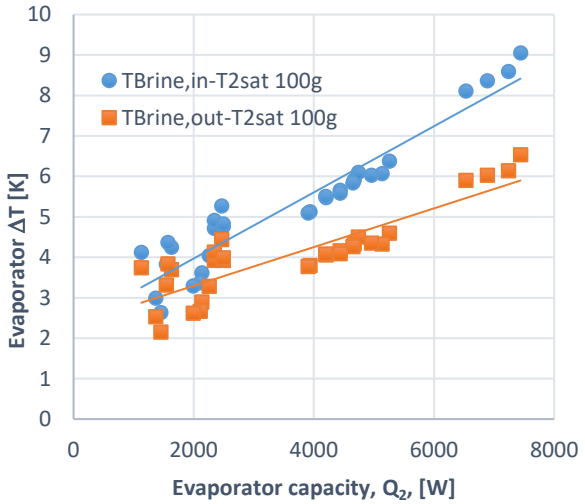

Figure 18. Water inlet and outlet temperature difference relative the saturation temperature at evaporator outlet vs cooling capacity. Different T_1 (in steps from about 30 to 57°C) and rpm (5985, 3015, 1485 and 990 rpm). Total charge 100 g.

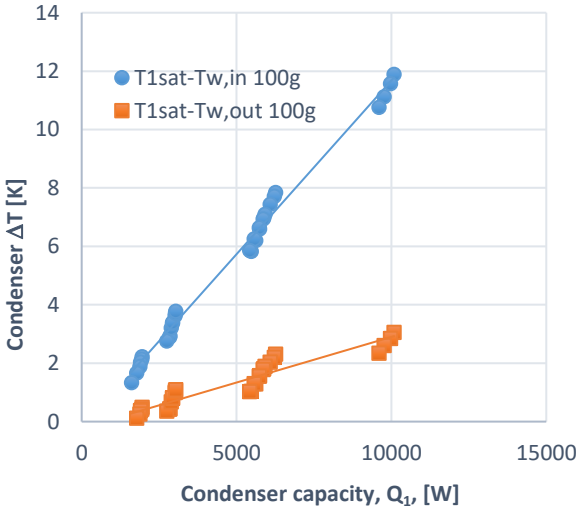

Figure 19. Water inlet and outlet temperature difference relative the saturation temperature at the condenser inlet vs heating capacity. Different T_1 (in steps from about 30 to 57°C) and rpm. (5985, 3015, 1485 and 990 rpm). Total charge 100 g.

Depending on the amount of oil in the system, problems with high pressure drop and poor heat transfer were noticed for the evaporator and SucHex. Using less than 50 g total oil charge kept these problems at a reasonable level.

Finally the compressor isentropic efficiency is illustrated in Figure 20. The compressor seems to be most efficient at 3000 rpm.

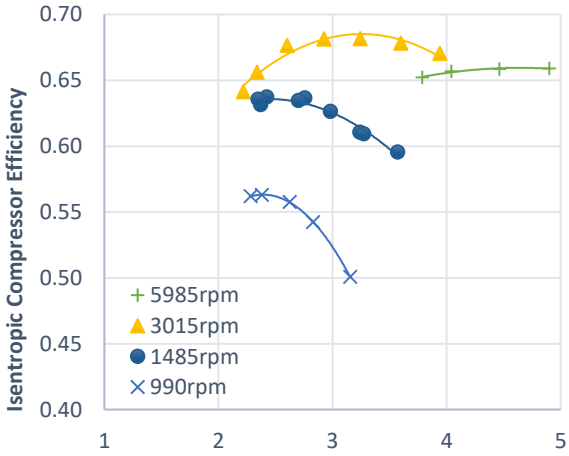

Figure 20. Compressor isentropic efficiency vs. p_1/p_2

5 CONCLUSIONS

It is possible to build a ground source heat pump with 10 kW heating capacity with 100 g refrigerant charge of propane.
It has been demonstrated that a wide range of capacity and water temperature conditions can be covered by the system.
The minimum charge required for the system is defined at the lowest capacity. Optimum charge at medium capacity seems to give excess of charge at maximum capacity. Using the specific charge, expressed as g/kW, as a figure of merit could therefore be misleading for comparison of this type of systems (IIR 25th info. note, 2014).
The optimum charge was checked at only one operation point. A more extensive analysis and more testing is required to define the optimum charge for a complete range of conditions in terms of capacity and water temperatures over a heating season.
The experiences from the development and testing of the evaporator and condenser indicate that further improvements are possible, both in terms of charge and performance.
The compressor tested has reasonable efficiency considering that all electronic losses are included and that it is not optimized for heat pump operating conditions. There is quite a pressure on car AC compressor manufactures to improve the efficiency and to adopt them also for heat pump operation. Still the life span is an issue. The choice of type of oil is another issue that need further investigations.

ACKNOWLEDGEMENTS

This project has been founded by the Swedish Energy Agency through the research program "Effsys Expand" and associated sponsor partners. Thanks!

NOMENCLATURE

T_1 = Refrigerant saturation temperature in condenser
T_2= Refrigerant saturation temperature in evaporator
p_1=Refrigerant saturation pressure in condenser
p_2= Refrigerant saturation pressure in evaporator
$COP_1 = Q_1/E_k$
$COP_2 = Q_2/E_k$

Q_1 = condenser capacity, Q_2 = evaporator capacity
E_k= compressor electric power (including rectifier and inverter drive elctronics)
x= vapor quality
ΔT_{sub}=Sub-cooling in condenser
ΔT=Temperature difference

REFERENCES

Fernando, W. P., Palm, B., Ameel, T., Lundqvist, P. & Granryd, E. (2008). A Minichannel Aluminium Tube Heat Exchanger - Part I-III: Evaluation of Single-Phase Heat Transfer Coefficients by the Wilson Plot Method. International journal of refrigeration, 31(4), 669-680, 681-695, 696-708.

Hughmark, G.A., 1962. Hold up in gas–liquid flow. Chemical Engineering Progress 58 (4), 62–65.

J. Acuña, P. Mogensen, B Palm. Evaluation of Coaxial Borehole Heat Exchanger Prototype. 14th ASME IHTC International Heat Transfer Conference, Washington D.C 2010.

Pavel Makhnatch, Gunda Mader. Refrigerants with low GWP and cost and energy efficiency optimization of vapor compression systems, Effsys Report, 2014

Refrigerant Charge Reduction, International Institute of Refrigeration, 25th Informatory Note on Refrigeration Technology